

Article

Fractional Coupling of Primary and Johari–Goldstein Relaxations in a Model Polymer

Carlo Andrea Massa ¹, Francesco Puosi ^{2,3} and Dino Leporini ^{1,3,*}

¹ Istituto per i Processi Chimico-Fisici-Consiglio Nazionale delle Ricerche (IPCF-CNR), Via G Moruzzi 1, 56124 Pisa, Italy

² Istituto Nazionale di Fisica Nucleare, Largo B. Pontecorvo 3, 56127 Pisa, Italy

³ Dipartimento di Fisica ‘Enrico Fermi’, Università di Pisa, Largo B. Pontecorvo 3, 56127 Pisa, Italy

* Correspondence: dino.leporini@unipi.it; Tel.: +39-050-2214937

Abstract: A polymer model exhibiting heterogeneous Johari–Goldstein (JG) secondary relaxation is studied by extensive molecular-dynamics simulations of states with different temperature and pressure. Time–temperature–pressure superposition of the primary (segmental) relaxation is evidenced. The time scales of the primary and the JG relaxations are found to be highly correlated according to a power law. The finding agrees with key predictions of the Coupling Model (CM) accounting for the decay in a correlation function due to the relaxation and diffusion of interacting systems. Nonetheless, the exponent of the power law, even if it is found in the range predicted by CM ($0 < \zeta < 1$), deviates from the expected one. It is suggested that the deviation could depend on the particular relaxation process involved in the correlation function and the heterogeneity of the JG process.

Keywords: polymer melt; Johari–Goldstein relaxation; dynamic heterogeneity; molecular-dynamics simulation



Citation: Massa, C.A.; Puosi, F.; Leporini, D. Fractional Coupling of Primary and Johari–Goldstein Relaxations in a Model Polymer. *Polymers* **2022**, *14*, 5560. <https://doi.org/10.3390/polym14245560>

Academic Editor: Aleksandar Y. Mehandzhiski

Received: 15 November 2022

Accepted: 15 December 2022

Published: 19 December 2022

Publisher’s Note: MDPI stays neutral with regard to jurisdictional claims in published maps and institutional affiliations.



Copyright: © 2022 by the authors. Licensee MDPI, Basel, Switzerland. This article is an open access article distributed under the terms and conditions of the Creative Commons Attribution (CC BY) license (<https://creativecommons.org/licenses/by/4.0/>).

1. Introduction

By lowering the temperature T or increasing the pressure P and avoiding crystallization, polymeric dense melts transform into a glass [1]. Close to the glass transition, relaxation occurs via both the primary (α) and the faster secondary (β) processes [2–4]. The β process has been intensively studied over the years [4–10].

In linear polymers, the secondary relaxation is due to the dynamics of the fragments of the chain [2,11–13] and considered a genuine manifestation of the Johari–Goldstein (JG) β relaxation [5]. The close relationship of the JG relaxation with the α relaxation has been noted [4,6,7,13,20–23], also due to the fact that both of them exhibit broad distribution of relaxation times [3,15,16] and cooperative dynamics [8,17,18].

It was early noted that the molecular reorganisation giving rise to the JG relaxation process is similar to those involved in the glass transition itself [19] with extensive later support [4,6,7,13,20–23]. It was concluded that the JG relaxation is a precursor to structural relaxation and viscous flow, with sluggish dynamics due to cooperativity driven by many body dynamics [6,8,15,18,24].

The several common features between JG and primary relaxation suggests that the secondary relaxation time τ_β and the primary relaxation time τ_α are correlated. This aspect has been widely investigated by the Coupling Model (CM) developed by Ngai and coworkers, who predicted the many-body effects in relaxation and diffusion of interacting systems [4]. CM focusses on the independent or primitive relaxation with time scale τ_0 . At times shorter than t_c ($t_c \simeq 2$ ps, insensitive to both the temperature T and the pressure P), the basic molecular units relax independently of each other and the correlation function $\phi(t)$ relaxes as an exponential with decay time τ_0 :

$$\phi(t) = \exp\left(-\frac{t}{\tau_0}\right) \quad t < t_c \quad (1)$$

For $t > t_c$, the intermolecular interactions slow down the α relaxation and the correlation function assumes the Kohlrausch–Williams–Watts (KWW) stretched exponential form ($0 < \beta \leq 1$):

$$\phi^{kww}(t) = \exp\left[-\left(\frac{t}{\tau}\right)^\beta\right] \quad t > t_c \quad (2)$$

with $\tau = \tau_\alpha$. The primitive relaxation is considered as precursor of the α relaxation, as expressed by the relation between their respective time scales:

$$\tau_0 = (t_c)^n (\tau_\alpha)^\beta \quad (3)$$

where $\beta = 1 - n$. Equation (3) follows from the requirement of continuity of $\phi(t)$, as given by Equations (1) and (2), at t_c and holds in the limit $t_c \ll \tau_0$ [4]. In many glass formers with genuine JG relaxations, it is found that, on changing both T and P , $\tau_0(T, P) \simeq \tau_\beta(T, P)$ [7]. Then, Equation (3) is finally recast as

$$\tau_\beta = (t_c)^n (\tau_\alpha)^\beta \quad (4)$$

Noticeably, Equation (4) predicts a power-law relation between τ_β and τ_α if the exponent β is constant, i.e., it does not depend on T and P . Given the generic form of the correlation function $\phi(t)$ assumed by CM, this conclusion has to be considered as independent of the particular relaxation process considered by $\phi(t)$. Equation (4) suggests that the JG relaxation and the primary relaxation are strongly correlated due to the intermolecular interactions whose influence becomes apparent for times exceeding t_c , a few picoseconds, i.e., much shorter than both τ_β and τ_α .

Close to the glass-transition spatial correlations between dynamic fluctuations—so-called dynamic heterogeneity (DH)—become apparent during the evolution of the α process [25–33]. Nonetheless, DH has been evidenced from picosecond [9] through β relaxation time scales [34–36], in agreement with previous suggestions [22].

The usual tool to characterize DH is the non-Gaussian parameter (NGP) [37]:

$$\alpha_2(t) = \frac{3}{5} \frac{\langle r^4(t) \rangle}{\langle r^2(t) \rangle^2} - 1 \quad (5)$$

where $r(t)$ is the modulus of the particle displacement in a time t . Brackets denote the ensemble average. NGP vanishes if the displacement is a spatially homogeneous single Gaussian-random process [38]. NGP has recently revealed the JG relaxation in metallic glasses [24] and polymers [36].

In this work, we report results from thorough molecular-dynamics (MD) simulations of a polymer model melt exhibiting strong DH of both the primary and JG relaxations, and constant stretching parameter β of the primary relaxation. Evidence is given of a power-law correlation between τ_β and τ_α . The finding is consistent with Equation (4). However, the exponent of the power law is found to be different from β .

2. Model and Numerical Methods

A dense melt of coarse-grained (bead-spring) linear polymer chains with $N_c = 512$ linear chains made of $M = 25$ monomers with mass m each, results in a total number of monomers $N = 12,800$ being studied by MD simulations [36]. Non-adjacent monomers in the same chain or monomers belonging to different chains are defined as “non-bonded” monomers. Non-bonded monomers at mutual distance r interact via a shifted Lennard–Jones (LJ) potential:

$$U^{LJ}(r) = \epsilon \left[\left(\frac{\sigma^*}{r} \right)^{12} - 2 \left(\frac{\sigma^*}{r} \right)^6 \right] + U_{cut}, \quad (6)$$

$\sigma^* = 2^{1/6}\sigma$ is the minimum of the potential, $U^{LJ}(r = \sigma^*) = -\epsilon + U_{cut}$. The potential is truncated at $r = r_c = 2.5\sigma$ and the constant U_{cut} adjusted to ensure that $U^{LJ}(r)$ is continuous at $r = r_c$ with $U^{LJ}(r) = 0$ for $r \geq r_c$. Along the same linear chain, monomers are bonded by the harmonic potential $U^{bond}(r) = k_{bond}(r - l_0)^2$, where the constant $k_{bond} = 2000\epsilon/\sigma^2$ to ensure high stiffness and the rest of the bond length $l_0 = 0.48\sigma$. A bending potential $U^{bend}(\alpha) = k_{bend}(\cos \alpha - \cos \alpha_0)^2$ ($k_{bend} = 2000\epsilon, \alpha_0 = 120^\circ$) ensures that the angle α between two consecutive bonds is nearly constant. The above model builds a torsional barrier when $l_0 < 0.5\sigma$ —as in the present work—which is discussed elsewhere [36]. Our chain model exhibits a significant local stiffness. In fact, the length ℓ_K of the associated Kuhn segment [39] is $\ell_K \sim 2$, larger than the one of flexible polymer model, such as the Kremer–Grest model with $\ell_K^{KG} \sim 1$ [40].

All the data presented in the work are expressed in reduced MD units: length in units of σ ; temperature in units of ϵ/k_B , where k_B is the Boltzmann constant; and time in units of $\tau_{MD} = (m\sigma^2/\epsilon)^{1/2}$. Roughly, $\tau_{MD} = 1$ corresponds to about 1 ps [41]. We set $\sigma = 1, \epsilon = 1, m = 1$ and $k_B = 1$.

Simulations were carried out with the open-source software LAMMPS [42,43]. Equilibration runs were performed at constant pressure P and temperature T (NPT ensemble) [44] (details about the barostat are found elsewhere [42,43]; the barostat damping parameter equals to 0.1 in MD time units). The investigated (P, T) pairs are listed in Table 1. It is worth nothing that, although some physical states ($P = 0; T = 0.85, 0.9, 0.95, 1.1$) were also considered elsewhere [36], the data reported in the present work have been produced independently, following the protocol mentioned above, so as to ensure maximum consistency and further support their robustness.

For each state, the equilibration was terminated not earlier than three times the end-to-end relaxation time [39]. Production runs were performed within the NVT ensemble [44]. Pressure was evaluated during all the production runs to monitor the full consistency with the pre-set value of the NPT equilibration run. Other details are given elsewhere [36].

Table 1. Investigated temperature and pressure values.

T \ p	0	0.5	1	1.5	2.5	5	7.5	10
1.1	◦	◦	◦		◦	◦	◦	◦
1	◦	◦	◦		◦	◦		
0.95	◦	◦	◦		◦	◦		
0.9	◦	◦	◦		◦	◦		
0.85	◦	◦	◦	◦	◦	◦		

3. Results

3.1. Bond Correlation Function

It has been demonstrated that the reorientation processes exhibit particular sensitivity to secondary motions [35,45–48]. From this respect, a convenient process is the reorientation of the chain bonds [35,48] with bond correlation function (BCF) [49]:

$$C(t) = \langle \cos \theta(t) \rangle \quad (7)$$

$\theta(t)$ is the angle spanned in a time t by the unit vector along a generic bond of a chain.

Figure 1 plots representative isothermal and isobaric decays of BCF. It exhibits an initial decay for $t \lesssim 1$ which is virtually independent of (P, T) . Then, a characteristic

two-step drop is apparent, evidencing two relaxation processes, i.e., the fast JG and the slow primary (segmental) relaxations [36,48,50,51].

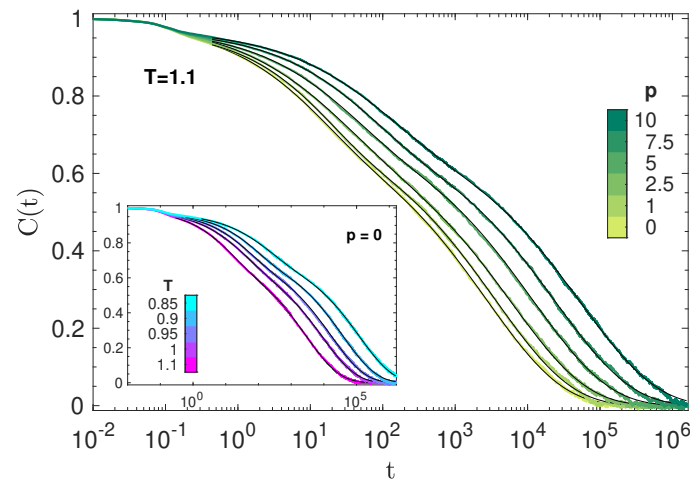


Figure 1. Isothermal and isobaric (inset) plots of selected BCFs, Equation (7). The superimposed thin solid black lines are the best fit with Equation (8).

3.2. Time Temperature and Pressure Superposition of Primary Relaxation

At long times, the shape of the BCF decay does not depend on the physical state. To show that, Figure 2 plots the master curve obtained by shifting the curves of Figure 1 horizontally, resulting in a remarkable time–temperature–pressure superposition (TTPS) in the time window of primary relaxation for $BCF(t^s) \lesssim 0.55$. The best fit of the master curve with the stretched exponential $A\phi^{kww}(t)$, where A is an adjustable constant, yields $\beta_{TTPS} = 0.415$.

TTPS motivated us to fit the whole BCF decay using different fit functions ensuring decay with constant stretching at long times. First, we adopted a weighted sum of two stretched exponentials, accounting for the primary (p) and the secondary (s) JG relaxation:

$$C(t) = \Delta_p \phi_p^{kww}(t) + \Delta_s \phi_s^{kww}(t) \tag{8}$$

where $\phi_i^{kww}(t)$, $i = p, s$ is Equation (2) with $\tau = \tau_i$, $\beta = \beta_i$. We set $\beta_p = \beta_{TTPS} = 0.415$ so as to leave Equation (8) with five adjustable parameters, i.e., $\Delta_p, \Delta_s, \tau_p, \tau_s, \beta_s$. The best-fit procedure yields excellent agreement, as shown in Figure 1.

Figure 2 shows that at short times in the JG time window, TTPS does not work. In fact, the best-fit procedure performed with Equation (8) returns stretching parameters of the JG relaxation which depend on the state and tend to decrease by slowing down the primary relaxation, see Figure 3.

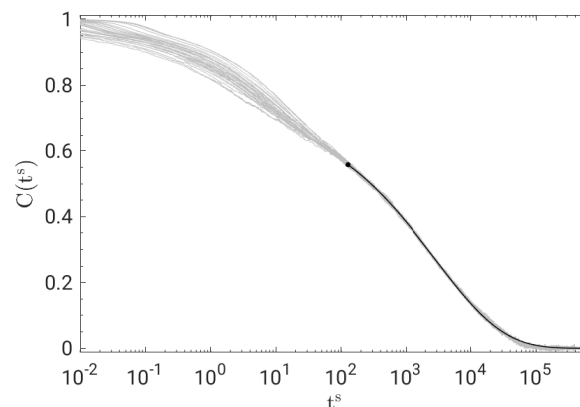


Figure 2. Time–temperature–pressure superposition (TTPS) of BCF for all the states in Figure 1.

The curves are shifted along the horizontal axis to optimise their superposition at long times. The superimposed solid black line is the best fit with a stretched exponential proportional to $\phi^{k_{JG}}(t)$, Equation (2), with $\beta_{TTPS} = 0.415$.

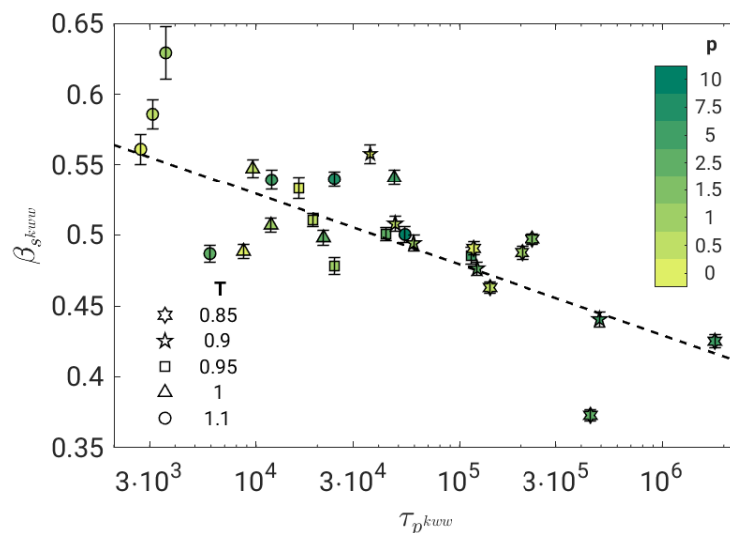


Figure 3. Stretching parameter of the secondary JG relaxation of all the investigated states according to the best fit with Equation (8). The dashed line is a guide for the eyes. Stretching increases mildly with the primary relaxation time.

3.3. Dynamic Heterogeneity

Figure 4 plots the NGP of the states in Figure 1 and shows how their DH develops with time. As in other studies, NGP is largely independent of (P, T) at very short times ($t \lesssim 0.1$), suggesting a major role of static structure [35]. The small peak at about 0.1 marks the average time between two consecutive collisions of the monomer with the cage formed by the closest neighbours [52]. For $t > 0.1$, NGP is strongly dependent on (P, T) . Two peaks are observed, the one occurring at a shorter time attributed to the JG heterogeneity whereas the one located at longer times are due to the familiar DH of the primary, structural relaxation [36]. The height of the NGP parameter in the JG region is not surprising, given the considerable stretching of the JG relaxation seen in Figure 3.

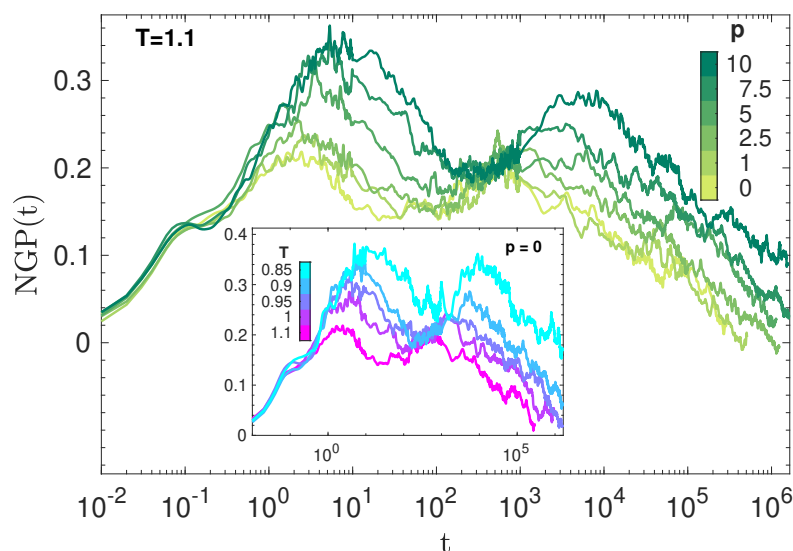


Figure 4. NGP, Equation (5), of all the states in Figure 1. DH is apparent in both the secondary JG relaxation time scale, $t \sim 1-10$, and the the primary, segmental relaxation, $t \sim 10^3-10^4$.

3.4. Fractional Coupling of Primary and JG Relaxations

We now test the possible correlation between the time scales of the primary, τ_p , and the secondary JG, τ_s , relaxation processes. Figure 5 shows the result by fitting the BCF in terms of Equation (8). The correlation is excellent (Pearson correlation coefficient $R = 0.998$) and well-expressed by a power law with exponent $\zeta = 0.71 \pm 0.01$.

To test the robustness of the result, we fit BCF with other functions with the same number of adjustable parameters. No significant changes were observed, i.e., τ_p and τ_s exhibit excellent power-law correlation with rather similar exponent. As an example, we considered the Williams ansatz [35,53–56]:

$$C(t) = [\Delta_p + \Delta_s \phi_s^{kww}(t)] \phi_p^{kww}(t) \tag{9}$$

which leads to $\zeta = 0.69 \pm 0.01$ ($R = 0.997$). Furthermore, following [16,35,55,56], we replaced ϕ_s^{kww} in Equation (8) with the Mittag–Leffler function:

$$\phi_s^{ml}(t) = E_a(- (t/\tau_s)) \tag{10}$$

with

$$E_a(x) = \sum_{k=0}^{\infty} \frac{x^k}{\Gamma(ak + 1)} \tag{11}$$

where $\Gamma(x)$ is the gamma function. This leads to $\zeta = 0.69 \pm 0.01$ ($R = 0.996$). If the same replacement is performed in Equation (9), we find $\zeta = 0.68 \pm 0.01$ ($R = 0.996$).

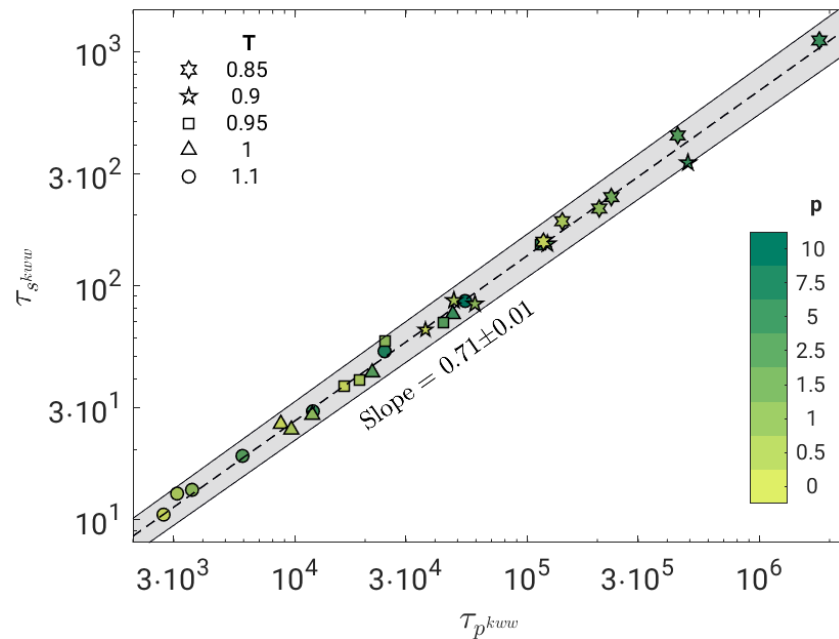


Figure 5. Correlation plot between the JG relaxation time τ_s and the primary relaxation time τ_p of all the investigated states, as drawn by fitting BCF $C(t)$ with a weighed superposition of two stretched exponentials, Equation (8). The correlation is excellent (Pearson correlation coefficient $R = 0.998$) and best fit with a power law with slope $\zeta = 0.71 \pm 0.01$ (dashed line). The grey area is the confidence region within one standard deviation of the best-fit parameters.

4. Discussion

The strong power-law correlation between the primary and the JG relaxation, evidenced by Figure 5, is the key result of the present work. The power-law coupling between different time scales in systems with significant DH is documented, a well-known example being the breakdown of the Stokes–Einstein relation [26,57].

The coupling model (CM) offers a highly investigated conceptual framework predicting, according to Equation (4), the fractional coupling between the JG and the primary relaxation. Notably, if TTPS holds, the stretching parameter β of the primary relaxation is independent of the (P, T) state and the fractional coupling reduces to a power law between τ_β and τ_α with exponent β ($0 < \beta \leq 1$). Indeed, the polymer model under study exhibits TTPS, Figure 2, and a power-law correlation between τ_β and τ_α in the investigated (P, T) range, Figure 5, with exponent $0 < \zeta < 1$. These findings are fully consistent with CM. However, the exponent of the power law ($\zeta = 0.71 \pm 0.01$) differs from the stretching parameter of the primary relaxation ($\beta_{\text{TTPS}} = 0.415$).

To the present level of understanding, the disagreement is not easily interpreted. We offer some tentative routes to be explored in future studies. First, notably, while the well-known phenomenon of DH on the time scale of the primary (structural) relaxation plays a central role in CM via the stretched relaxation, Equation (2), the influence of much less investigated DH on the JG time scale, which is evidenced in the present and previous studies [36], is not apparent in CM. Furthermore, we notice that CM is quite generic, i.e., the predictions are *independent* of the relaxation process involved in the correlation function $\phi(t)$. However, if the torsional autocorrelation function is studied by MD simulations of a polymer model which is rather similar to the present one, one finds a power law between JG and primary relaxation with an exponent $\zeta_{BS} \sim 0.25$ (see Figure 7 in ref. [51]), which is almost three times less than ours ($\zeta = 0.71 \pm 0.01$) by considering BCF. This finding suggests that, even if the power-law coupling is robust, i.e., it is revealed by different correlation functions, and captured by CM, the exponent ζ of the power law and the stretching β could depend on the particular relaxation process in a different way. Unfortunately, no information about the possible TTPS and the stretching parameter of the primary relaxation is given in ref. [51], thus hampering a closer comparison with the present study. We noted elsewhere that BCF is more sensitive to the JG relaxation than the torsional autocorrelation function in the polymer model of the present study [48].

The influence of both the choice of the correlation function, as well as the magnitude of DH in JG relaxation, on the observation of the fractional coupling between the primary and the JG relaxation is postponed to future systematic studies.

5. Conclusions

A polymer model exhibiting heterogeneous JG secondary relaxation was studied by extensive MD simulations of states with different temperature and pressure. The TTPS of the primary (segmental) relaxation is evidenced. The time scales of the primary and the JG relaxations are found to be highly correlated according to a power law in agreement with CM predictions. Nonetheless, the exponent of the power law, even if it is in the CM range ($0 < \zeta < 1$), deviates from the expected one. This motivates further investigation of the particular relaxation process involved in the correlation function addressed by CM and the heterogeneity of the JG process.

Author Contributions: Conceptualization, C.A.M., F.P. and D.L.; methodology, validation, formal analysis, investigation, C.A.M., F.P. and D.L.; software, C.A.M. and F.P.; writing—review and editing, C.A.M., F.P. and D.L.; supervision, F.P. and D.L. All authors have read and agreed to the published version of the manuscript.

Funding: A generous grant of computing time from Green Data Center of the University of Pisa, and Dell EMC® Italia is gratefully acknowledged. F.P. acknowledges funding from the European Union's Horizon 2020 research and innovation programme under the Marie Skłodowska-Curie grant agreement No. 754496.

Institutional Review Board Statement: Not applicable.

Informed Consent Statement: Not applicable.

Data Availability Statement: The data presented in this study are available on request from the corresponding author.

Acknowledgments: Gianfranco Cordella and Antonio Tripodo are warmly thanked for helpful discussions.

Conflicts of Interest: The authors declare no conflict of interest.

Abbreviations

The following abbreviations are used in this manuscript:

BCF	Bond correlation function
CM	Coupling model
DH	Dynamical heterogeneity
JG	Johari–Goldstein
KWW	Kohlrausch–Williams–Watts
LJ	Lennard–Jones
MD	Molecular dynamics
NGP	Non-Gaussian parameter
NPT	Constant number of monomers N , constant pressure P and constant temperature T
NVT	Constant number of monomers N , constant volume V and constant temperature T
TTPS	Time–temperature–pressure superposition

References

1. Debenedetti, P.G. *Metastable Liquids*; Princeton University Press: Princeton, NJ, USA, 1997.
2. McCrum, N.G.; Read, B.E.; Williams, G. *Anelastic and Dielectric Effects in Polymeric Solids*; Dover Publications: New York, NY, USA, 1991.
3. Angai, C.A.; Ngai, K.L.; McKenna, G.B.; McMillan, P.; Martin, S.W. Relaxation in glassforming liquids and amorphous solids. *J. Appl. Phys.* **2000**, *88*, 3113–3157. [[CrossRef](#)]
4. Ngai, K.L. *Relaxation and Diffusion in Complex Systems*; Springer: Berlin/Heidelberg, Germany, 2011.
5. Johari, G.P.; Goldstein, M. Viscous Liquids and the Glass Transition. II. Secondary Relaxations in Glasses of Rigid Molecules. *J. Chem. Phys.* **1970**, *53*, 2372. [[CrossRef](#)]
6. Ngai, K.L. Relation between some secondary relaxations and the α relaxations in glass-forming materials according to the coupling model. *J. Chem. Phys.* **1998**, *109*, 6982–6994. [[CrossRef](#)]
7. Ngai, K.L.; Paluch, M. Classification of secondary relaxation in glass-formers based on dynamic properties. *J. Chem. Phys.* **2004**, *120*, 857–873. [[CrossRef](#)]
8. Capaccioli, S.; Paluch, M.; Prevosto, D.; Wang, L.M.; Ngai, K.L. Many-Body Nature of Relaxation Processes in Glass-Forming Systems. *J. Phys. Chem. Lett.* **2012**, *3*, 735–743. [[CrossRef](#)]
9. Cicerone, M.T.; Zhong, Q.; Tyagi, M. Picosecond Dynamic Heterogeneity, Hopping, and Johari-Goldstein Relaxation in Glass-Forming Liquids. *Phys. Rev. Lett.* **2014**, *113*, 117801. [[CrossRef](#)]
10. Yu, H.-B.; Richert, R.; Samwer, K. Structural rearrangements governing Johari-Goldstein relaxations in metallic glasses. *Sci. Adv.* **2017**, *3*, 1701577. [[CrossRef](#)]
11. Boyd, R.H.; Breitling, S.M. The Conformational Analysis of Crankshaft Motions in Polyethylene. *Macromolecules* **1974**, *7*, 855–862. [[CrossRef](#)]
12. Paul, W.; Smith, G.D.; Yoon, D.Y. Static and Dynamic Properties of a n-C100H202 Melt from Molecular Dynamics Simulations. *Macromolecules* **1997**, *30*, 7772–7780. [[CrossRef](#)]
13. Meier, R.J.; Struik, L. Atomistic modelling study of relaxation processes in polymers: The β -relaxation in polyvinylchloride. *Polymer* **1998**, *39*, 31–38. [[CrossRef](#)]
14. Goldstein, M. The past, present, and future of the Johari–Goldstein relaxation. *J. Non-Cryst. Solids* **2011**, *357*, 249–250. . [[CrossRef](#)]
15. Johari, G.P. Source of JG-Relaxation in the Entropy of Glass. *J. Phys. Chem. B* **2019**, *123*, 3010–3023. . 10.1021/acs.jpcc.9b00612. [[CrossRef](#)]
16. Smith, G.D.; Bedrov, D. Relationship between the α - and β -relaxation processes in amorphous polymers: Insight from atomistic molecular dynamics simulations of 1,4-polybutadiene melts and blends. *J. Polym. Sci. Part B Polym. Phys.* **2007**, *45*, 627–643.
17. Karmakar, S.; Dasgupta, C.; Sastry, S. Short-Time Beta Relaxation in Glass-Forming Liquids Is Cooperative in Nature. *Phys. Rev. Lett.* **2016**, *116*, 085701. [[CrossRef](#)]
18. Ngai, K.L.; Capaccioli, S.; Paluch, M.; Wang, L. Clarifying the nature of the Johari-Goldstein β -relaxation and emphasising its fundamental importance. *Philos. Mag.* **2020**, *100*, 2596–2613. [[CrossRef](#)]
19. Johari, G.P. Glass Transition and Secondary Relaxations in Molecular Liquids and Crystals. *Ann. N. Y. Acad. Sci.* **1976**, *279*, 117–140.
20. Bershtein, V.; Egorov, V.; Egorova, L.; Ryzhov, V. The role of thermal analysis in revealing the common molecular nature of transitions in polymers. *Thermochim. Acta* **1994**, *238*, 41–73. . [[CrossRef](#)]
21. Böhmer, R.; Diezemann, G.; Geil, B.; Hinze, G.; Nowaczyk, A.; Winterlich, M. Correlation of Primary and Secondary Relaxations in a Supercooled Liquid. *Phys. Rev. Lett.* **2006**, *97*, 135701. [[CrossRef](#)]

22. Goldstein, M. Communications: Comparison of activation barriers for the Johari–Goldstein and alpha relaxations and its implications. *J. Chem. Phys.* **2010**, *132*, 041104.
23. Cicerone, M.T.; Tyagi, M. Metabasin transitions are Johari–Goldstein relaxation events. *J. Chem. Phys.* **2017**, *146*, 054502. [[CrossRef](#)]
24. Wang, B.; Zhou, Z.Y.; Guan, P.F.; Yu, H.B.; Wang, W.H.; Ngai, K.L. Invariance of the relation between α relaxation and β relaxation in metallic glasses to variations of pressure and temperature. *Phys. Rev. B* **2020**, *102*, 094205. [[CrossRef](#)]
25. Sillescu, H. Heterogeneity at the glass transition: A review. *J. Non-Cryst. Solids* **1999**, *243*, 81–108. [[CrossRef](#)]
26. Ediger, M.D. Spatially heterogeneous dynamics in supercooled liquids. *Annu. Rev. Phys. Chem.* **2000**, *51*, 99–128. [[CrossRef](#)]
27. Richert, R. Heterogeneous dynamics in liquids: Fluctuations in space and time. *J. Phys. Condens. Matter* **2002**, *14*, R703–R738. [[CrossRef](#)]
28. Berthier, L.; Biroli, G. Theoretical perspective on the glass transition and amorphous materials. *Rev. Mod. Phys.* **2011**, *83*, 587–645. [[CrossRef](#)]
29. Karmakar, S.; Dasgupta, C.; Sastry, S. Length scales in glass-forming liquids and related systems: A review. *Rep. Prog. Phys.* **2015**, *79*, 016601. [[CrossRef](#)]
30. Tracht, U.; Wilhelm, M.; Heuer, A.; Feng, H.; Schmidt-Rohr, K.; Spiess, H.W. Length Scale of Dynamic Heterogeneities at the Glass Transition Determined by Multidimensional Nuclear Magnetic Resonance. *Phys. Rev. Lett.* **1998**, *81*, 2727–2730. [[CrossRef](#)]
31. Colmenero, J.; Alvarez, F.; Arbe, A. Self-motion and the α relaxation in a simulated glass-forming polymer: Crossover from Gaussian to non-Gaussian dynamic behavior. *Phys. Rev. E* **2002**, *65*, 041804. [[CrossRef](#)]
32. Napolitano, S.; Capponi, S.; Vanroy, B. Glassy dynamics of soft matter under 1D confinement: How irreversible adsorption affects molecular packing, mobility gradients and orientational polarization in thin films. *Eur. Phys. J. E* **2013**, *36*, 61. [[CrossRef](#)]
33. Napolitano, S.; Glynos, E.; Tito, N.B. Glass transition of polymers in bulk, confined geometries, and near interfaces. *Rep. Prog. Phys.* **2017**, *80*, 036602. [[CrossRef](#)]
34. Weeks, E.R.; Crocker, J.C.; Levitt, A.C.; Schofield, A.; Weitz, D.A. Three-Dimensional Direct Imaging of Structural Relaxation Near the Colloidal Glass Transition. *Science* **2000**, *287*, 627–631.
35. Fragiadakis, D.; Roland, C.M. Role of structure in the α and β dynamics of a simple glass-forming liquid. *Phys. Rev. E* **2017**, *95*, 022607. [[CrossRef](#)] [[PubMed](#)]
36. Puosi, F.; Tripodo, A.; Malvaldi, M.; Leporini, D. Johari–Goldstein Heterogeneous Dynamics in a Model Polymer. *Macromolecules* **2021**, *54*, 2053–2058. [[CrossRef](#)]
37. Hansen, J.P.; McDonald, I.R. *Theory of Simple Liquids*, 3rd ed.; Academic Press: New York, NY, USA, 2006.
38. Zorn, R. Deviation from Gaussian behavior in the self-correlation function of the proton motion in polybutadiene. *Phys. Rev. B* **1997**, *55*, 6249–6259. [[CrossRef](#)]
39. Doi, M.; Edwards, S.F. *The Theory of Polymer Dynamics*; Clarendon Press: Oxford, UK, 1988.
40. Kremer, K.; Grest, G.S. Dynamics of entangled linear polymer melts: A molecular-dynamics simulation. *J. Chem. Phys.* **1990**, *92*, 5057–5086. [[CrossRef](#)]
41. Kröger, M. Simple models for complex nonequilibrium fluids. *Phys. Rep.* **2004**, *390*, 453–551. [[CrossRef](#)]
42. Plimpton, S. Fast Parallel Algorithms for Short-Range Molecular Dynamics. *J. Comput. Phys.* **1995**, *117*, 1–19. [[CrossRef](#)]
43. Available online: <http://lammmps.sandia.gov> (accessed on 30 October 2022).
44. Allen, M.P.; Tildesley, D.J. *Computer Simulations of Liquids*, 2nd ed.; Oxford University Press: Oxford, UK, 2017.
45. Richter, D.; Monkenbusch, M.; Arbe, A.; Colmenero, J.; Farago, B. Dynamic structure factors due to relaxation processes in glass-forming polymers. *Phys. B Condens. Matter* **1997**, *241–243*, 1005–1012. [[CrossRef](#)]
46. Tölle, A. Neutron scattering studies of the model glass former *ortho*-terphenyl. *Rep. Prog. Phys.* **2001**, *64*, 1473–1532. [[CrossRef](#)]
47. Fragiadakis, D.; Roland, C.M. Dynamic correlations and heterogeneity in the primary and secondary relaxations of a model molecular liquid. *Phys. Rev. E* **2014**, *89*, 052304. [[CrossRef](#)]
48. Tripodo, A.; Puosi, F.; Malvaldi, M.; Capaccioli, S.; Leporini, D. Coincident Correlation between Vibrational Dynamics and Primary Relaxation of Polymers with Strong or Weak Johari–Goldstein Relaxation. *Polymers* **2020**, *12*, 761. [[CrossRef](#)] [[PubMed](#)]
49. Barbieri, A.; Campani, E.; Capaccioli, S.; Leporini, D. Molecular dynamics study of the thermal and the density effects on the local and the large-scale motion of polymer melts: Scaling properties and dielectric relaxation. *J. Chem. Phys.* **2004**, *120*, 437–453. [[CrossRef](#)] [[PubMed](#)]
50. Bedrov, D.; Smith, G.D. Molecular dynamics simulation study of the α and β -relaxation processes in a realistic model polymer. *Phys. Rev. E* **2005**, *71*, 050801. [[CrossRef](#)] [[PubMed](#)]
51. Bedrov, D.; Smith, G.D. Secondary Johari–Goldstein relaxation in linear polymer melts represented by a simple bead-necklace model. *J. Non-Cryst. Solids* **2011**, *357*, 258–263. [[CrossRef](#)]
52. De Michele, C.; Leporini, D. Viscous flow and jump dynamics in molecular supercooled liquids. I. Translations. *Phys. Rev. E* **2001**, *63*, 036701. [[CrossRef](#)]
53. Williams, G. Molecular aspects of multiple dielectric relaxation processes in solid polymers. In Proceedings of the Electric Phenomena in Polymer Science. In *Advances in Polymer Science*; Springer: Berlin/Heidelberg, Germany, 1979; pp. 59–92.
54. Williams, G. Dielectric relaxation spectroscopy of polymers revealing dynamics in isotropic and anisotropic stationary systems and changes in molecular mobility in non-stationary systems. *Polymer* **1994**, *35*, 1915–1922. [[CrossRef](#)]

-
55. Fragiadakis, D.; Roland, C.M. Characteristics of the Johari-Goldstein process in rigid asymmetric molecules. *Phys. Rev. E* **2013**, *88*, 042307. [[CrossRef](#)]
 56. Fragiadakis, D.; Roland, C.M. Rotational dynamics of simple asymmetric molecules. *Phys. Rev. E* **2015**, *91*, 022310. [[CrossRef](#)]
 57. Chang, I.; Fujara, F.; Geil, B.; Heuberger, G.; Mangel, T.; Sillescu, H. Translational and rotational molecular motion in supercooled liquids studied by NMR and forced Rayleigh scattering. *J. Non-Cryst. Solids* **1994**, *172–175*, 248–255. [[CrossRef](#)]